Electronic Supplementary Material (ESI) for Dalton Transactions
This journal is © The Royal Society of Chemistry 2012

Supporting information

From well-defined Pt(II) surface species to the controlled growth of silica supported Pt nanoparticles

Pierre Laurent,[a,b] Laurent Veyre,[a] Chloé Thieuleux,[a] Sébastien Donet,[b] and Christophe Copéret[a,c]

a Université de Lyon, Institut de Chimie de Lyon, UMR C2P2 - CNRS - Université Lyon 1-ESCPE Lyon, Equipe Chimie Organométallique de Surface 43, Bd du 11 Novembre 1918 F-69616 Villeurbanne, France.

b CEA, LITEN, Département des Technologies des Nanomatériaux, Laboratoire des Technologies de Surfaces (LTS), 17, Rue des Martyrs, 38054 Grenoble, France

c Present address: ETH Zürich, Department of Chemistry, Laboratory of Inorganic Chemistry, Wolfgang Pauli Strasse 10, CH-8093, Zürich, Switzerland.

This journal is © The Royal Society of Chemistry 2012

A. Analytical techniques

Solid State Nuclear Magnetic Resonance Spectroscopy

^{1}H magic angle spinning (MAS) and ^{13}C cross polarization (CP)-MAS solid-state NMR spectra were recorded on a Brüker Avance III 500 MHz spectrometer with a conventional double resonance 4 mm CP-MAS probe operating respectively at 500 MHz for 1H and 125 MHz for 13C. The samples were introduced under Ar in a zirconia rotor, which was then tightly closed. In all experiments, the rotation frequency was set to ca. 10 kHz. For cross polarization experiments the contact time was set to 2 ms. Chemical shifts are given with respect to TMS as external references for ^{1}H and ^{13}C NMR (0 ppm).

TEM microscopy

All samples for TEM analysis were prepared under air by directly dipping the TEM grids into the powder samples to avoid the use of any solvent associated with the risk of aggregating or leaching of the nanoparticles. A Philips CM120 Transmission Electron Microscope was used at the Centre Technologique des Microstructures Université Lyon 1, the acceleration voltage was set to 120 kV.

Direct Reflectance Infrared Fourier Transform Spectroscopy (DRIFT).

Infrared spectra were recorded on a Nicolet Magna 550 FT spectrometer using a custom infrared cell equipped with CaF_2 windows, allowing in situ studies. Typically, 64 scans were accumulated for each spectrum (resolution 4 cm^{-1}). The reflectance measurements were refined according to the Kubelka-Munk theory for enhanced resolution. Samples are loaded under argon in a glove box.

This journal is © The Royal Society of Chemistry 2012

B. Single Crystal X-Ray diffraction

Table S-1.

	(COD)Pt(Me)(OSi(O*t*Bu)$_3$) (**2**)	(COD)Pt(OSi(O*t*Bu)$_3$)(N(SiMe)$_3$) (**3**)
Formula	$C_{21}H_{42}PtO_4Si$	$C_{26}H_{57}NPtO_4Si_3$
Formula weight (g.mol^{-1})	581.74	727.09
Crystal size (mm)	0.38x0.21x0.13	0.63x0.53x0.45
Color, morphology	coloreless	light yellow
ρ (g.cm^{-3})	1.563	1.452
Lattice type, crystal system	Monoclinic	Triclinic
Space group	$P2_1/n$	P -1
Z	2	2
Cell constant		
a (Å)	9.465(1)	10.5195(5)
b (Å)	8.6144(9)	11.5936(6)
c (Å)	30.436(3)	14.5167(8)
α (°)	90	72.425(5)
β (°)	95.187(9)	80.632(4)
γ (°)	90	89.822(4)
V (Å^3)	2471.4(4)	1663.3(2)
F_{000}	1168	744
μ (Mo Kα) (mm^{-1})	5.75	4.36
θ (°)	3.6-29.5	3.5-29.5
Scan type	ω scans	ω scans
Temperature (K)	150	150
Measured reflections	22806	43516
Refinement	full least-square matrix on F^2	full least-square matrix on F^2
Independent relections	6069	8476
No. Parameters	244	317
$R[F^2>2\sigma(F^2)]/ wR_2$	0.047/ 0.149	0.031/ 0.066
GoF	0.99	1
Max peak in final diff. map (e- Å^{-3})	2.09	1.86
Min peak in final diff. map (e- Å-3)	-3.57	-1.76

This journal is © The Royal Society of Chemistry 2012

C. (COD)Pt(Me)$_2$

Figure S1. IR-DRIFT

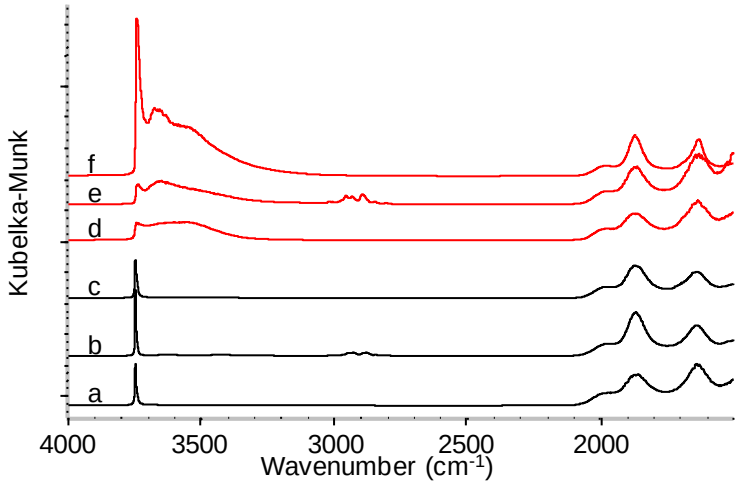

a) $SiO_{2\text{-}700,}$ b) (COD)Pt(Me)$_2$@$SiO_{2\text{-}700}$, c) after static H_2 treatment, d) $SiO_{2\text{-}200}$, e) (COD)Pt(Me)$_2$@$SiO_{2\text{-}200}$, f) after static H_2 treatment

	grafted	after H_2
$SiO_{2\text{-}700}$	3057/3001/2945/2927/2877/2842/2801	-
$SiO_{2\text{-}200}$	3018/3005/2955/2930/2894/2648/2802	-

Figure S2.

Solid-state NMR of (COD)Pt(Me)$_2$@SiO2$_{-200}$

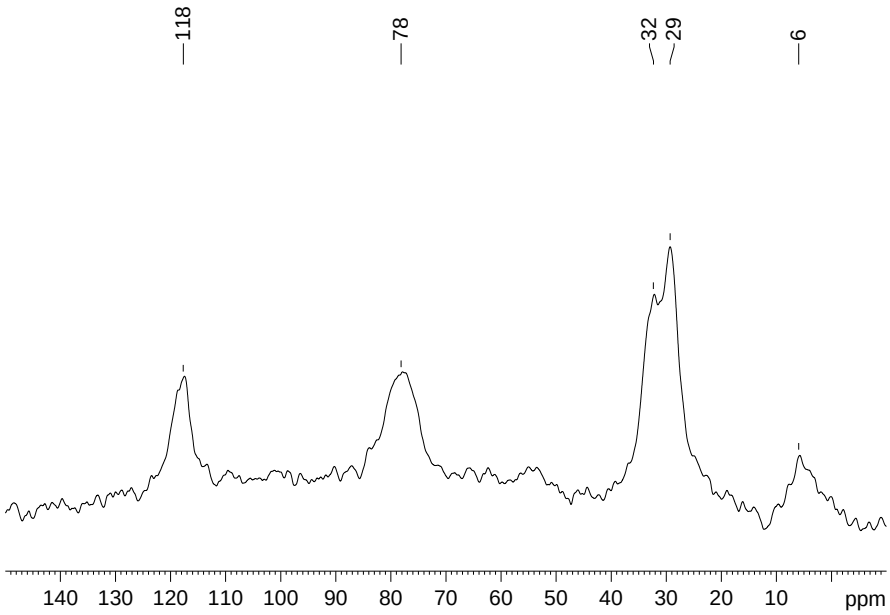

^{13}C CP/MAS solid state NMR spectra of (COD)Pt(Me)$_2$@SiO$_{2\text{-}200}$ (d1 = 6 s, 10484 scans, lb=100Hz)

Solid-state NMR of (COD)Pt(Me)$_2$@SiO$_{2\text{-}700}$

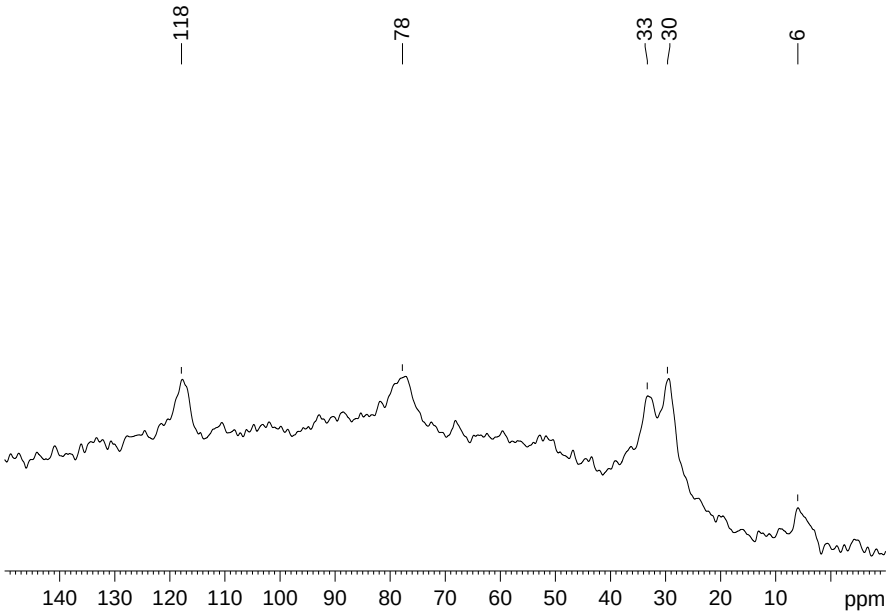

^{13}C CP/MAS solid state NMR spectra of (COD)Pt(Me)$_2$@SiO$_{2\text{-}700}$ (d1 = 4 s, 33702 scans, lb=100Hz)

Solid-state NMR of (COD)Pt(Me)$_2$ mixed in the solid state with SiO$_{2\text{-}700}$

This journal is © The Royal Society of Chemistry 2012

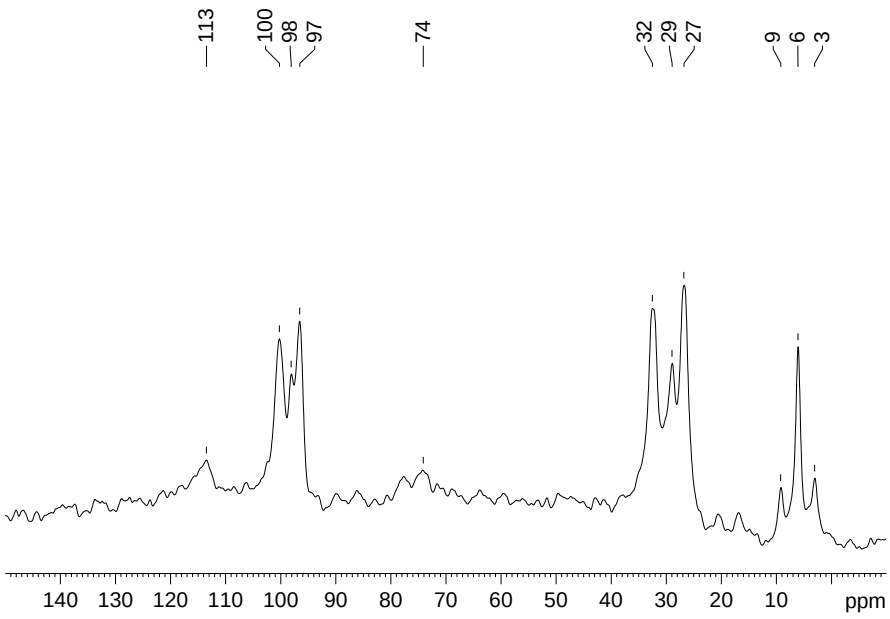

^{13}C CP/MAS solid state NMR spectra of (COD)Pt(Me)$_2$ + SiO$_{2\text{-}700}$ (d1 = 2 s, 3433 scans, lb=100Hz)

Figure S3. TEM

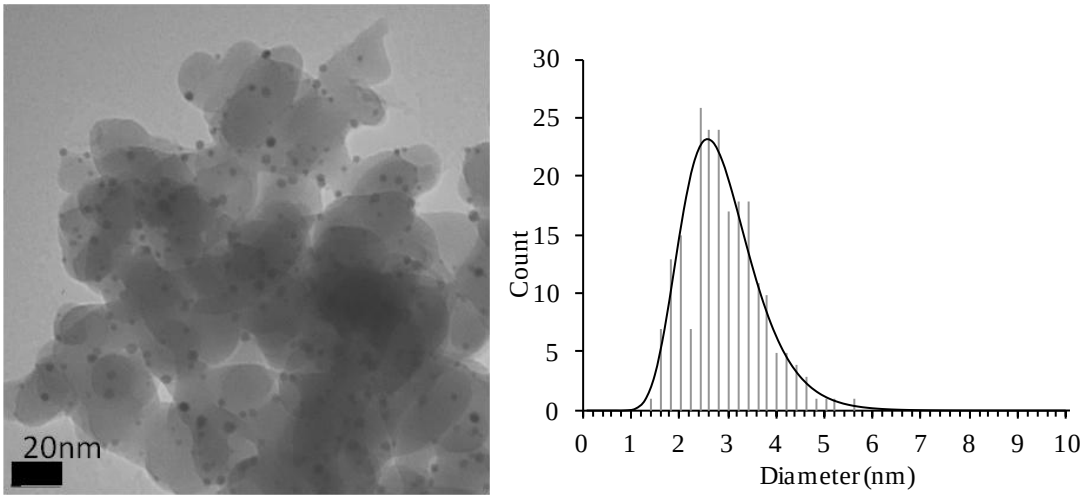

(COD)Pt(Me)$_2$@SiO$_{2\text{-}200}$ treated under static H_2 atmosphere. 170 nanoparticles count. Mean size 3.0 (σ=0.7) nm.

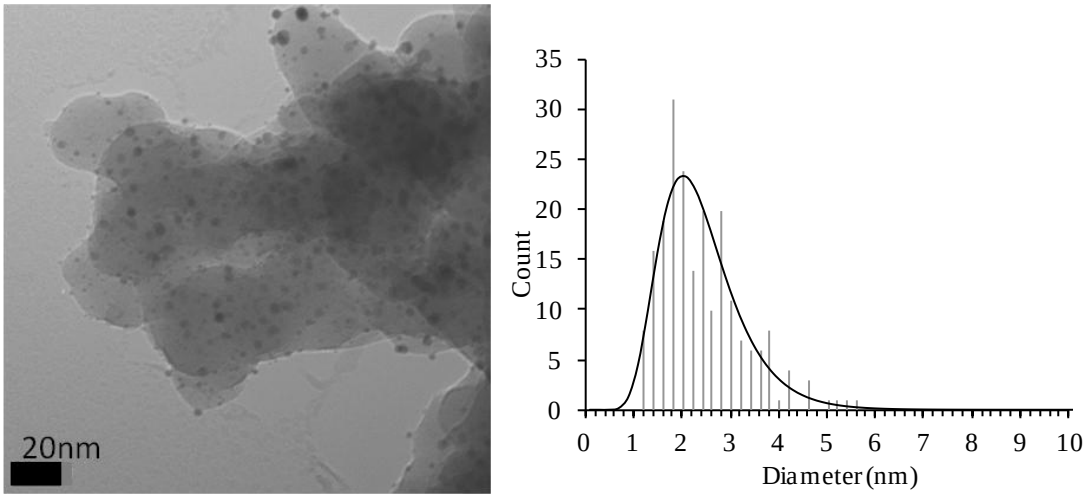

(COD)Pt(Me)$_2$@SiO$_{2\text{-}700}$ treated under static H2 atmosphere. 212 nanoparticles count. Mean size 2.4 (σ=0.9) nm.

This journal is © The Royal Society of Chemistry 2012

D. (COD)Pt(OSi(O*t*Bu)$_3$)$_2$

Figure S4. IR-DRIFT

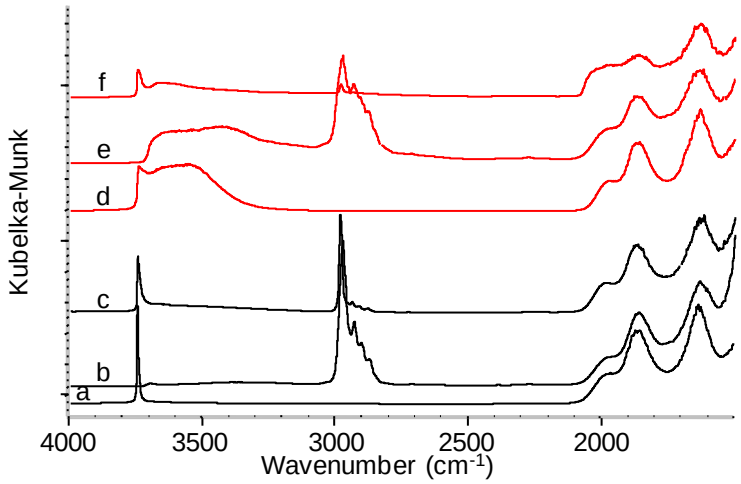

a) $SiO_{2\text{-}700,}$ b) (COD)Pt(OSi(OtBu)$_3$)$_2$@$SiO_{2\text{-}700}$, c) after static H_2 treatment, d) $SiO_{2\text{-}200}$, e) (COD)Pt(OSi(OtBu)$_3$)$_2$@$SiO_{2\text{-}200}$, f) after static H_2 treatment

	grafted	after H_2
$SiO_{2\text{-}700}$	3370/2975/2933/2905/2876	2982/2955/2938/2913/2880
$SiO_{2\text{-}200}$	3420/2975/2931/2905/2876/2850	2984/2040

This journal is © The Royal Society of Chemistry 2012

Figure S5.

Solid-state NMR of (COD)Pt(OSi(OtBu)$_3$)$_2$@SiO$_{2\text{-}200}$

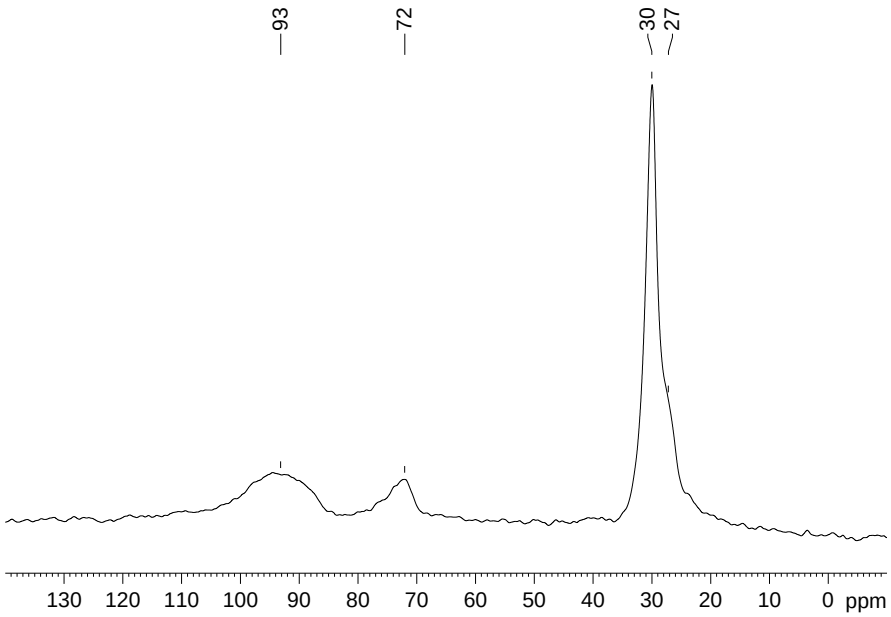

13C CP/MAS solid state NMR spectra of (COD)Pt(OSi(OtBu)$_3$)$_2$@SiO$_{2\text{-}200}$ (d1 = 4 s, 12766 scans, lb=100Hz)

Solid-state NMR of (COD)Pt(OSi(OtBu)$_3$)$_2$@SiO$_{2\text{-}700}$

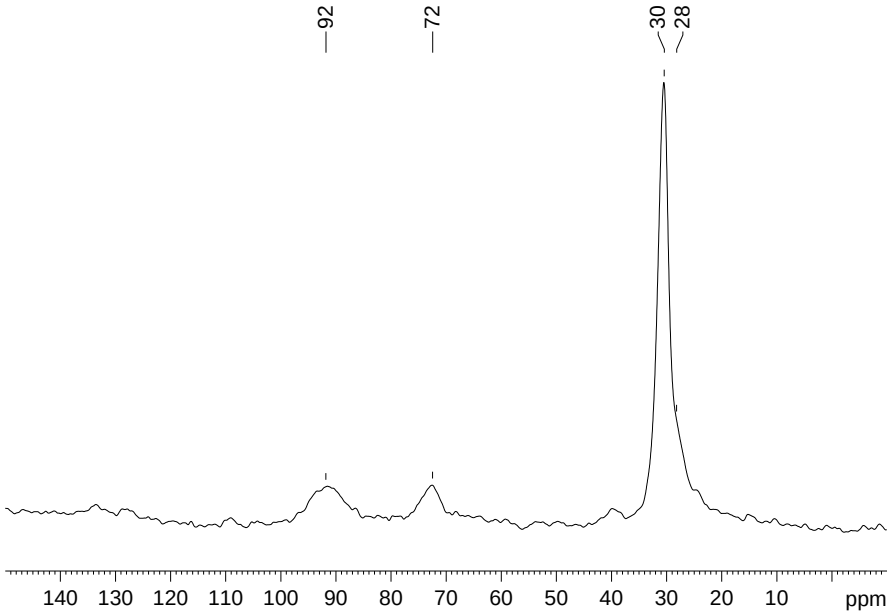

13C CP/MAS solid state NMR spectra of (COD)Pt(OSi(O*t*Bu)$_3$)$_2$@SiO$_{2\text{-}700}$ (d1 = 2 s,2618 scans, lb=50Hz)

Figure S6. TEM

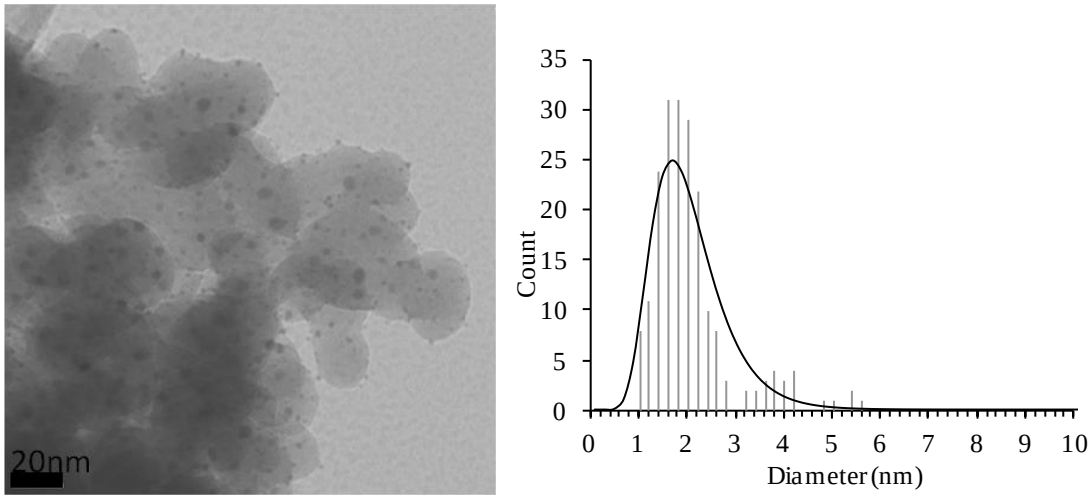

(COD)Pt(OSi(O*t*Bu)$_3$)$_2$@SiO$_{2\text{-}200}$ treated under static H_2 atmosphere. 200 nanoparticles count.

Mean size 2.1 (σ=0.9) nm.

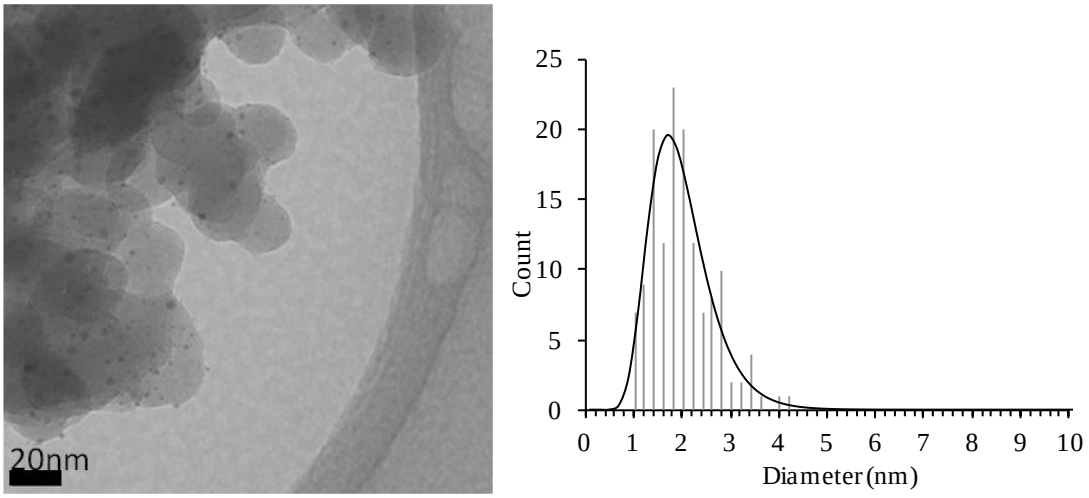

(COD)Pt(OSi(OtBu)$_3$)$_2$@SiO$_{2\text{-}700}$ treated under static H_2 atmosphere. 200 nanoparticles count.

Mean size 2.0 (σ=0.6) nm.

This journal is © The Royal Society of Chemistry 2012

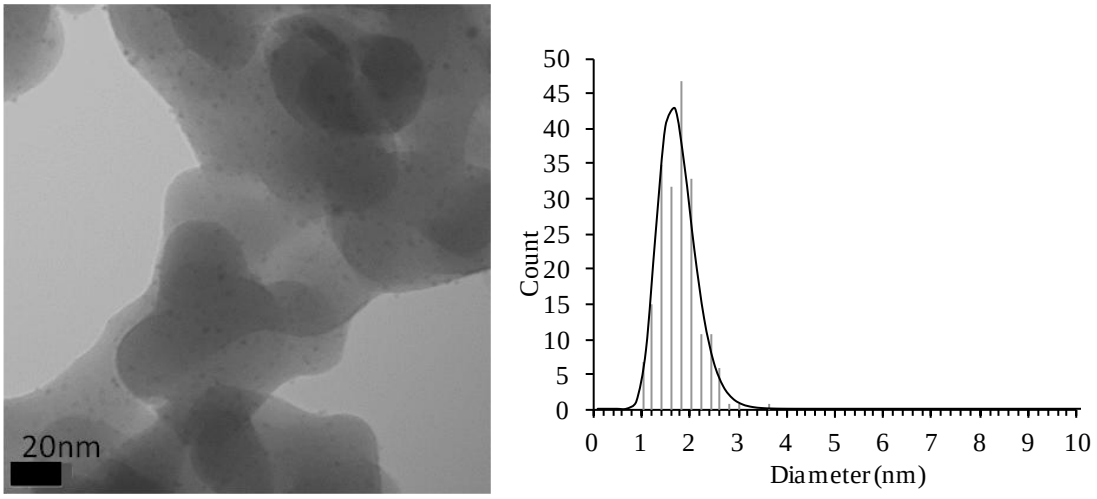

$(COD)Pt(OSi(OtBu)_3)_2@SiO_{2\text{-}700}$ treated under H_2 flow. 200 nanoparticles count. Mean size 1.8 (σ=0.4) nm.

E. (COD)Pt(Me)(OSi(O*t*Bu)$_3$)

Figure S7.

Liquid NMR of 2 (COD)Pt(Me)(OSi(OtBu)$_3$) in C_6D_6.

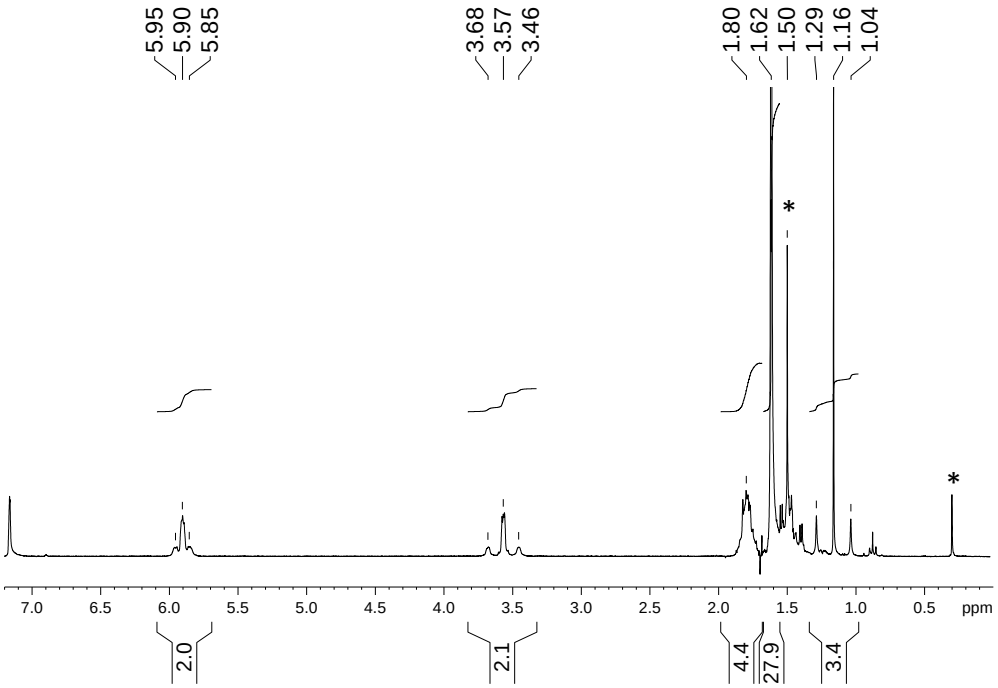

^{1}H NMR, d1=1sec, 8 scans.

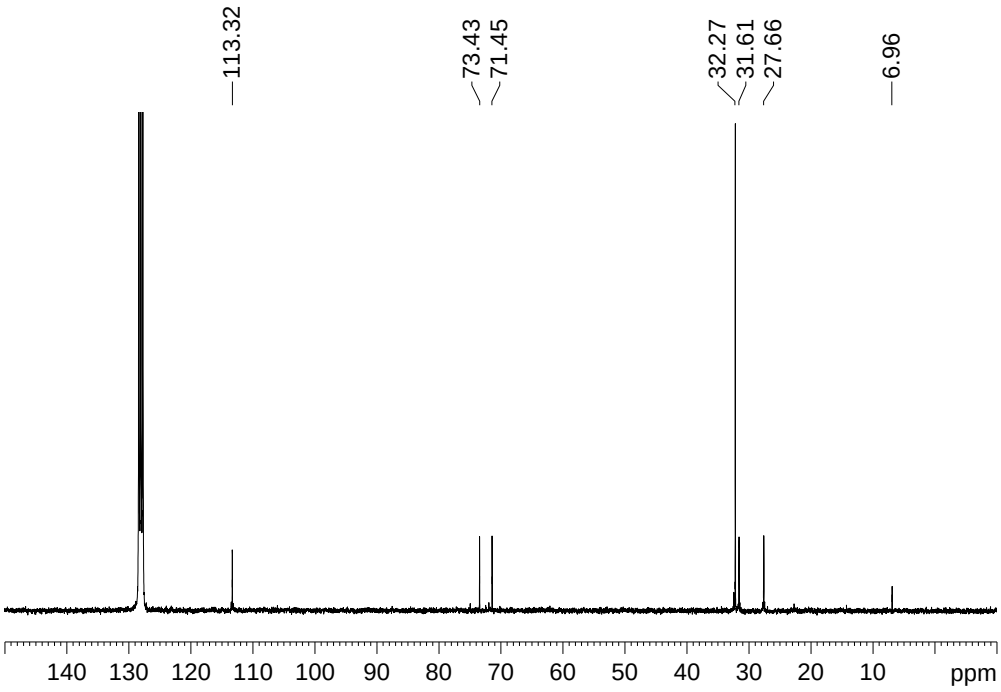

^{13}C NMR in C6D6, d1=1sec, 17709 scans

^{1}H NMR (C_6D_6; δ, ppm): 1.16 (t, 3H, C*H*$_3$, JPt-H=75Hz), 1.50 (m, 4H, endo C*H*$_2$), 1.62 (s, 27H, OC*Me*$_3$), 1.80 (m, 4H, exo C*H*$_2$), 3.57 (t, 2H, =C*H*, trans to OSi, JPt-H=66 Hz), 5.90 (t, 2H, =C*H*, trans to CH_3, JPt-H=30Hz).
^{13}C NMR (C_6D_6; δ, ppm): 6.9 (s, *C*H_3, JPt-C=700 Hz), 27.6 (s, *C*H_2), 31.6 (s, *C*H_2), 32.2 (s, OC*Me*$_3$), 71.4 (s, O*C*Me_3), 73.4 (s, =CH, trans to OSi, JPt-C=227 Hz), 113.3 (s, =CH, trans to CH_3, JPt-C=26.5 Hz).

Figure S8. IR-DRIFT

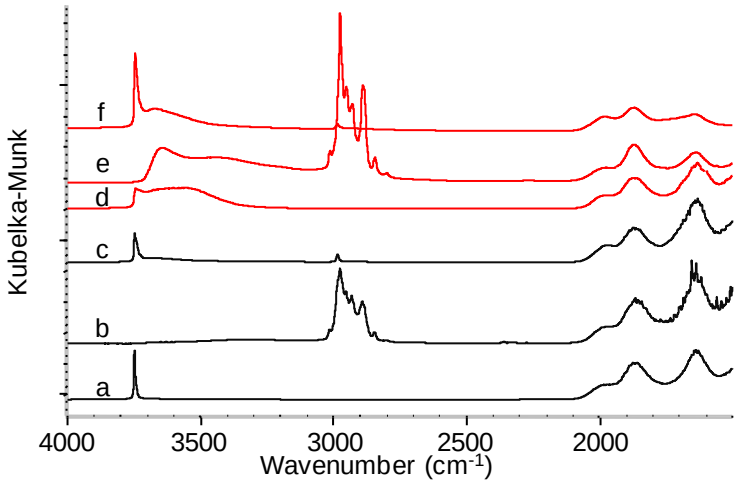

a) $SiO_{2\text{-}700}$, b) (COD)Pt(Me)(OSi(OtBu)$_3$)@$SiO_{2\text{-}700}$, c) after static H_2 treatment, d) $SiO_{2\text{-}200}$, e) (COD)Pt(Me)(OSi(OtBu)$_3$)@$SiO_{2\text{-}200}$, f) after static H_2 treatment

	grafted	after H_2
$SiO_{2\text{-}700}$	3015/2977/2954/2932/2893/2888/2846/2800	2983
$SiO_{2\text{-}200}$	3413/3013/2975/2951/2928/2890/2844/2801	2984

This journal is © The Royal Society of Chemistry 2012

Figure S9.

Solid-state NMR of (COD)Pt(Me)(OSi(OtBu)$_3$@SiO$_{2\text{-}200}$

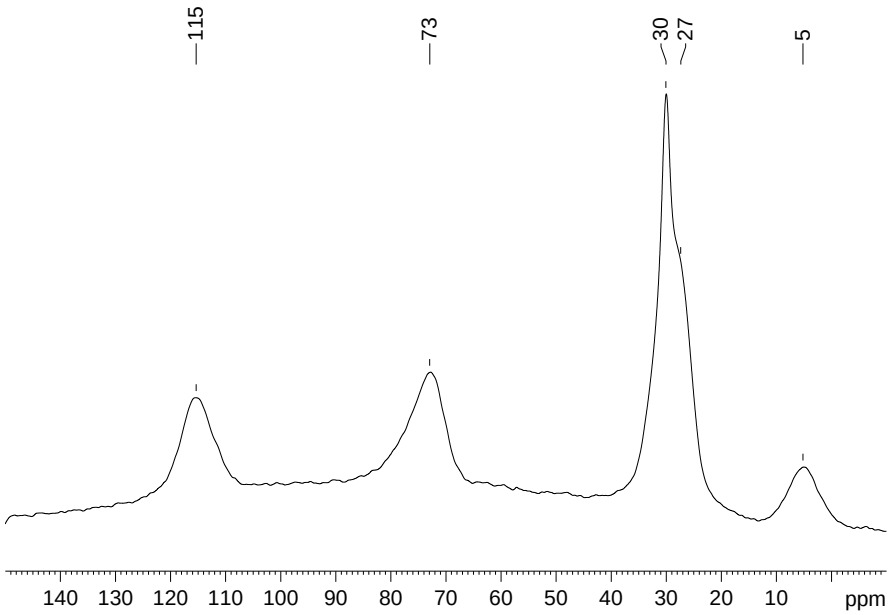

13C CP/MAS solid state NMR spectra of (COD)Pt(Me)(OSi(O*t*Bu)$_3$)@SiO$_{2\text{-}200}$ **(**d1 = 2 s, 100000 scans, lb=100Hz)

Solid-state NMR of CODPt(Me)(OSi(OtBu)$_3$)@SiO$_{2\text{-}700}$

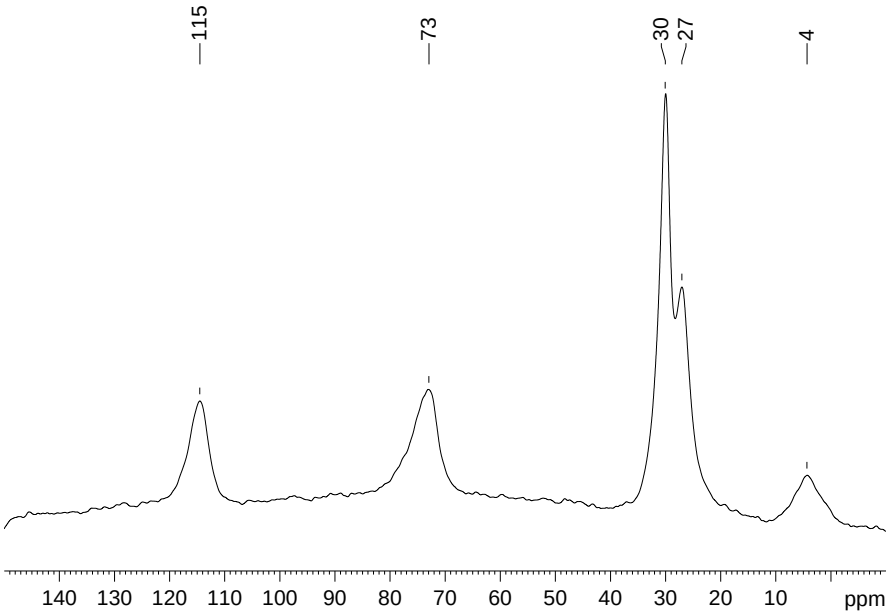

^{13}C CP/MAS solid state NMR spectra of (COD)Pt(Me)((OSi(O*t*Bu)$_3$)@SiO$_{2\text{-}700}$ (d1 = 6 s, 38069 scans, lb=100Hz)

Figure S10. TEM

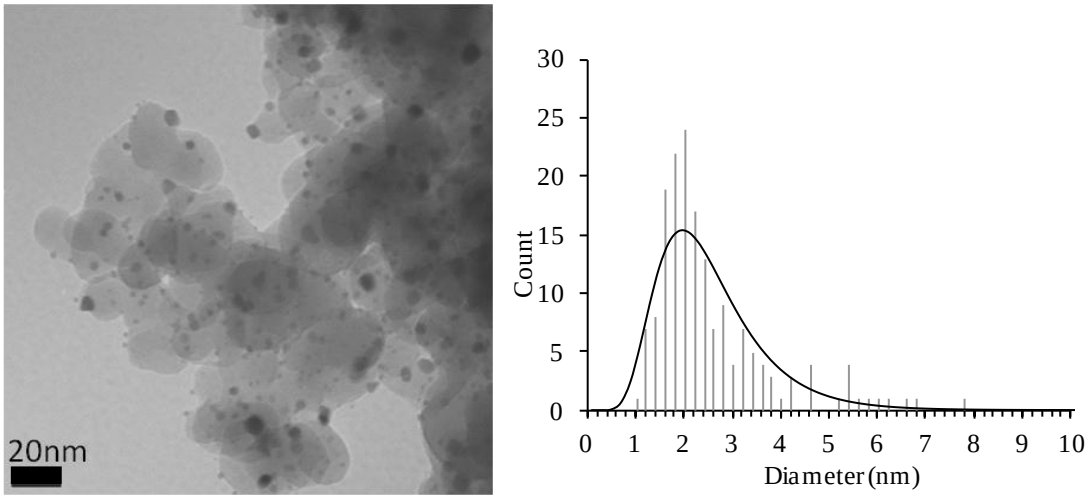

(COD)Pt(Me)((OSi(O*t*Bu)$_3$)@SiO$_{2\text{-}200}$ treated under static H_2. 170 nanoparticles count. Mean size 2.6 (σ=1.2) nm.

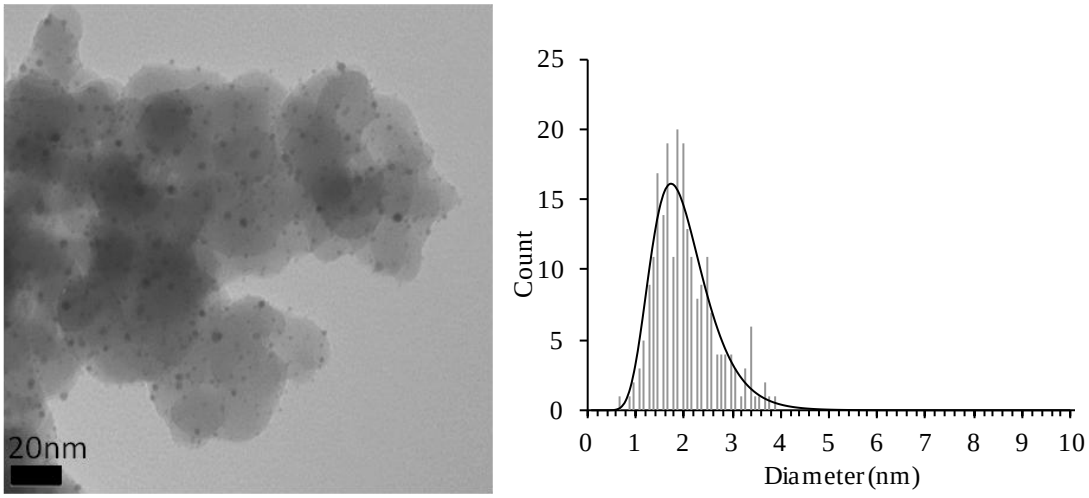

(COD)Pt(Me)(OSi(O*t*Bu)$_3$)/SiO$_{2\text{-}700}$ treated under static H_2. 226 nanoparticles count. Mean size 2.0 (σ=0.6) nm.

F. (COD)Pt(Me)N(SiMe$_3$)$_2$

Figure S11. Liquid NMR of 1 (COD)Pt(Me)N(SiMe$_3$)$_2$ in C$_6$D$_6$.

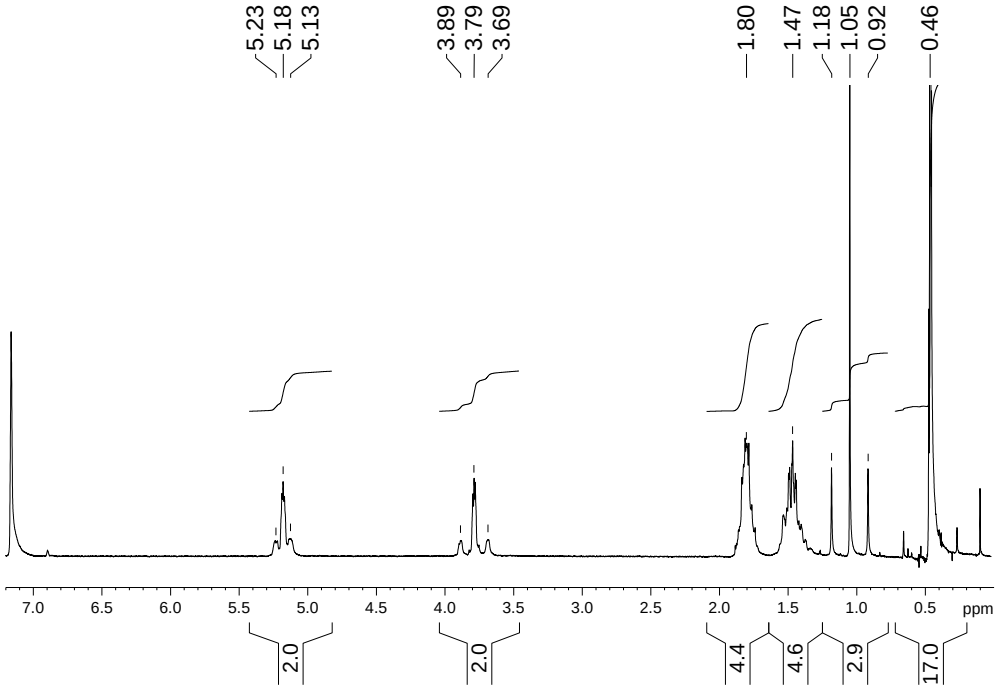

^{1}H NMR, d1=1sec, 8 scans.

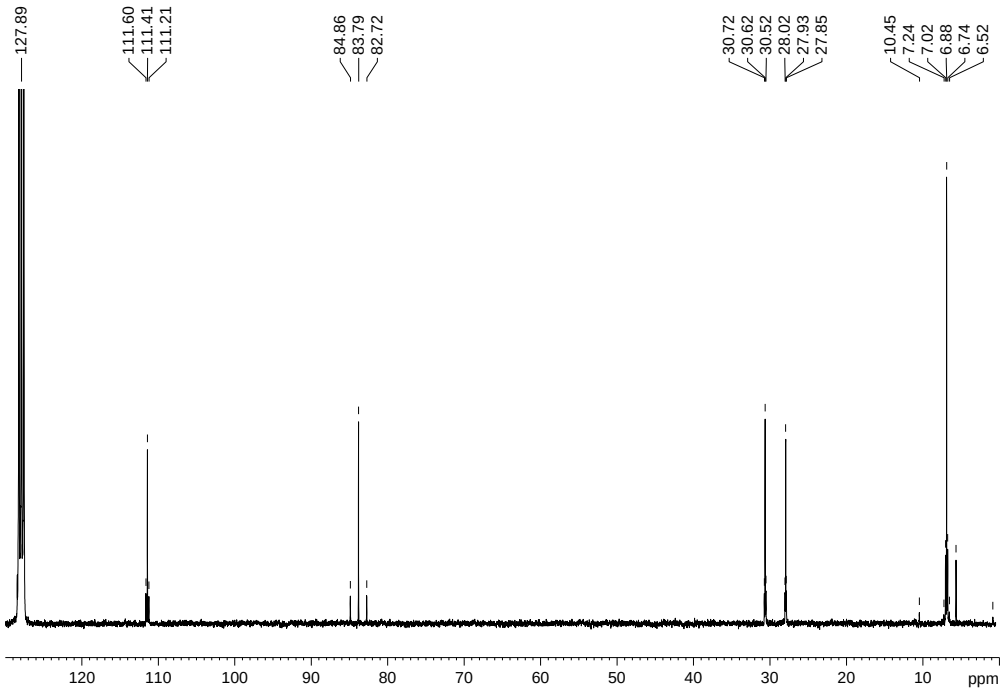

^{13}C NMR, d1=1sec, 10000 scans

^{1}H NMR (C6D6; δ, ppm): 0.46 (s, 18H, -Si*Me$_3$*), 1.05 (t, 3H, Pt-C*H$_3$*, JPt-H=80Hz), 1.47 (m, 4H, endo C*H$_2$*), 1.80 (m, 4H, exo C*H$_2$*), 3.79 (t, 2H, =C*H*, trans to N, JPt-H=60 Hz), 5.18 (t, 2H, =C*H*, trans to CH$_3$, JPt-H=30Hz).

^{13}C NMR (C6D6; δ, ppm): 5.8 (t, *C*CH_3, Me, JPt-C=726.8 Hz), 6.8 (m, Si*C*H3), 28.1 (t, *C*H_2, JPt-C=12.9 Hz), 30.8 (t, *C*H_2, JPt-C=15.9 Hz), 83.9 (t, =*C*H, trans to N, JPt-C=161.3 Hz), 111.6 (s, =*C*H, trans to CH_3, JPt-C=29.4 Hz).

Figure S12. IR-DRIFT

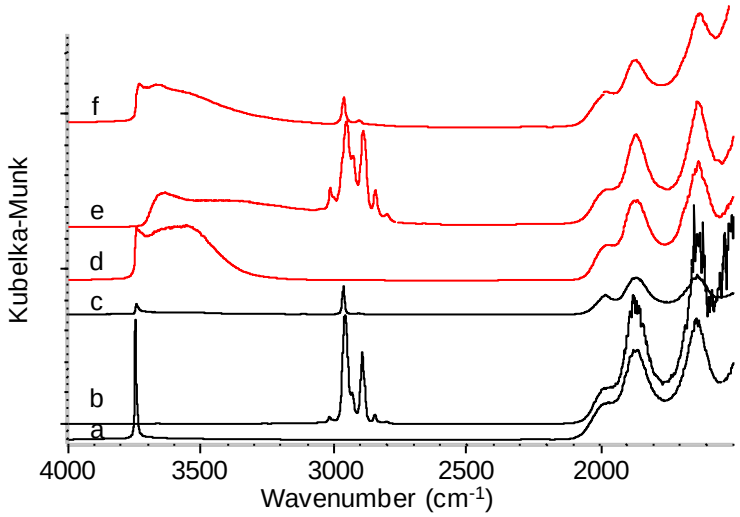

a) $SiO_{2\text{-}700}$, b) (COD)Pt(Me)($N(SiMe_3)_2$)@$SiO_{2\text{-}700}$, c) after static H_2 treatment, d) $SiO_{2\text{-}200}$, e) (COD)Pt(Me)($N(SiMe_3)_2$)@$SiO_{2\text{-}200}$, f) after static H_2 treatment

	grafted	after H_2
$SiO_{2\text{-}700}$	3017/3002/2962/2957/2932/2895/2846/2802	3747/2966//2907/1980
$SiO_{2\text{-}200}$	3014/3000/2954/2927/2890/2844/2796	2965/2905/1982

Figure S13.

Solid-state NMR of (COD)Pt(Me)(N(SiMe$_3$)$_2$)@SiO$_{2\text{-}200}$

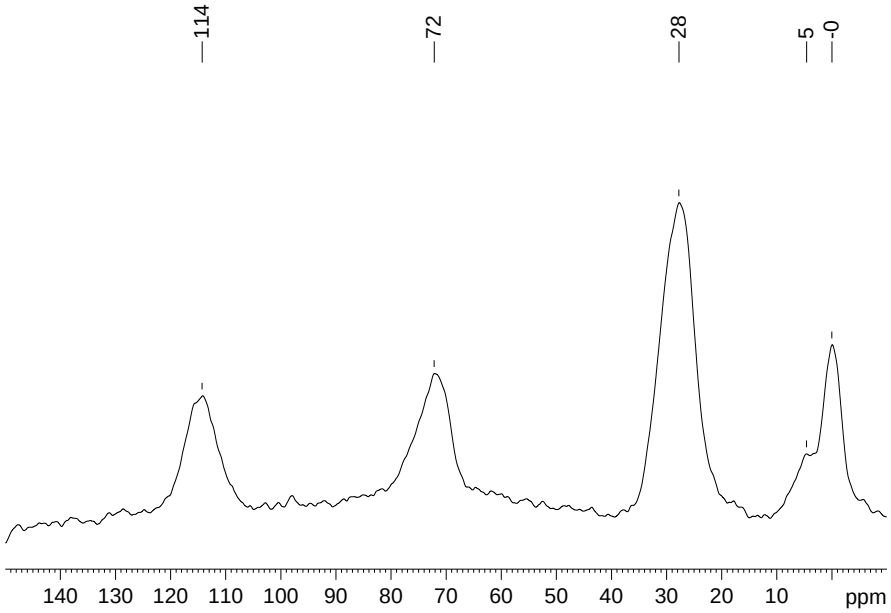

^{13}C CP/MAS solid state NMR spectra of (COD)Pt(Me)(N(SiMe$_3$)$_2$)/SiO$_{2\text{-}(200)}$ (d1 = 2 s, 26482 scans, lb=100Hz)

Solid-state NMR of (COD)Pt(Me)N(SiMe$_3$)$_2$@SiO$_{2\text{-}700}$

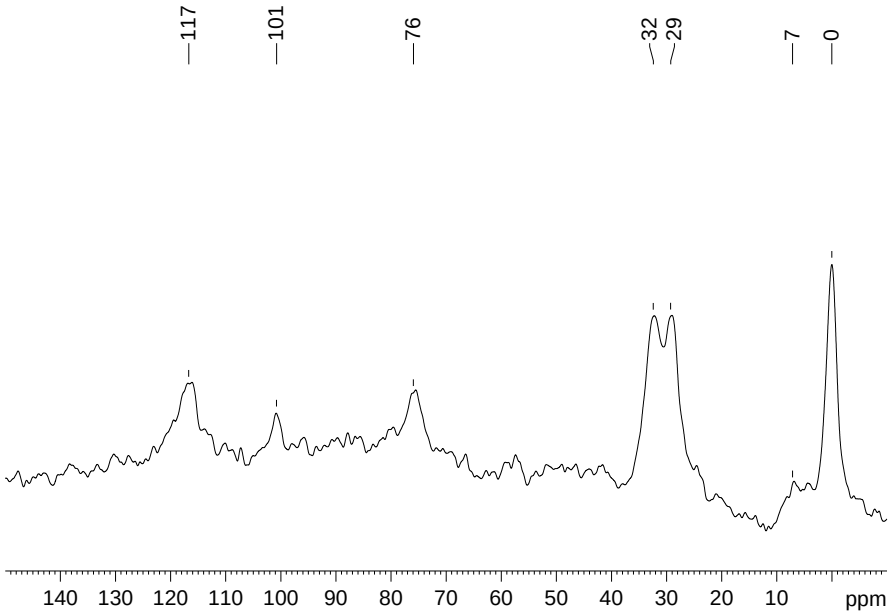

^{13}C CP/MAS solid state NMR spectra of (COD)Pt(Me)(N(SiMe$_3$)$_2$)@SiO$_{2\text{-}700}$ (d1 = 2 s, 10379 scans, lb=100Hz)

This journal is © The Royal Society of Chemistry 2012

Figure S14. TEM

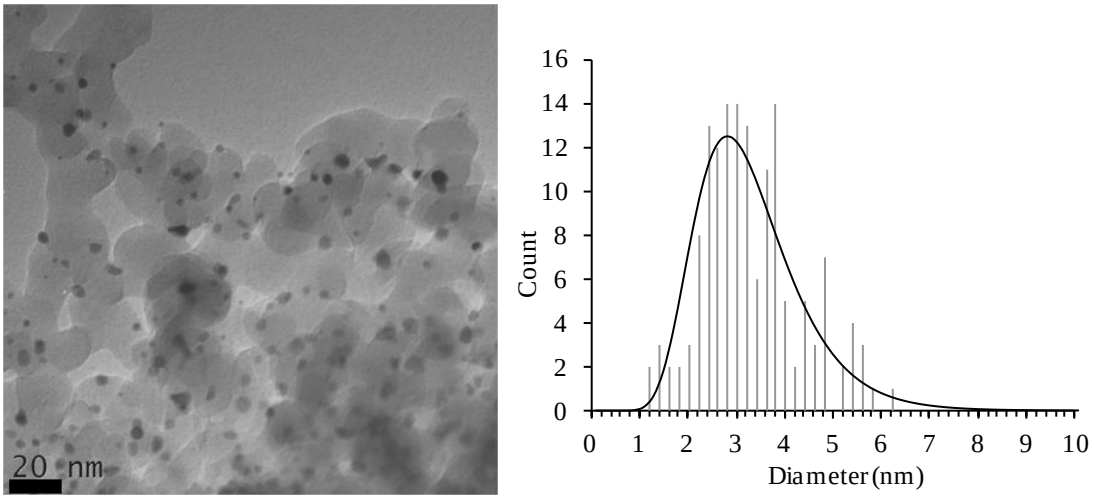

(COD)Pt(Me)(N(SiMe$_3$)$_2$)@SiO$_{2\text{-}200}$ treated under static H_2. 150 nanoparticles count. Mean size 3.3 (σ=1.0) nm.

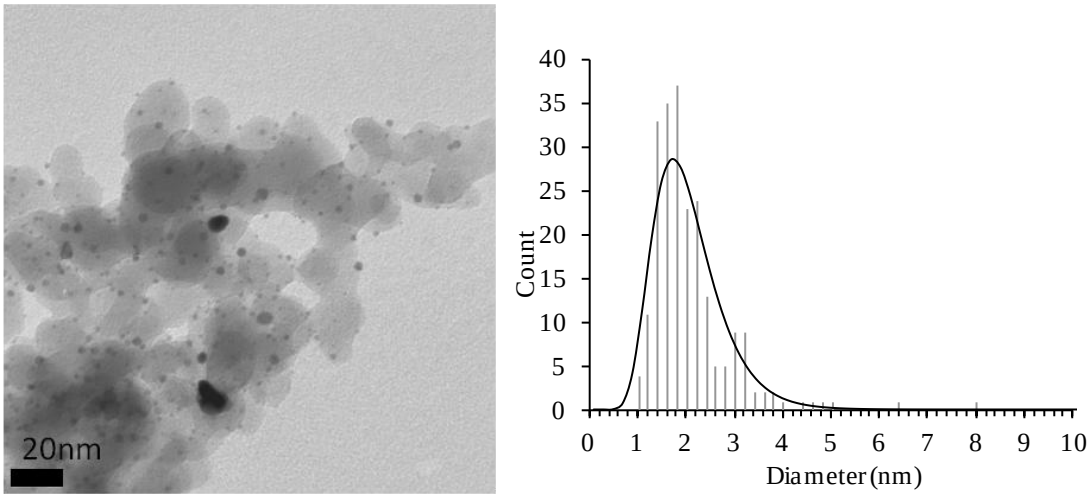

(COD)Pt(Me)(N(SiMe$_3$)$_2$)@SiO$_{2\text{-}700}$ treated under static H_2 atmosphere. 221 nanoparticles count. Mean size 2.1 (σ=0.9) nm.

This journal is © The Royal Society of Chemistry 2012

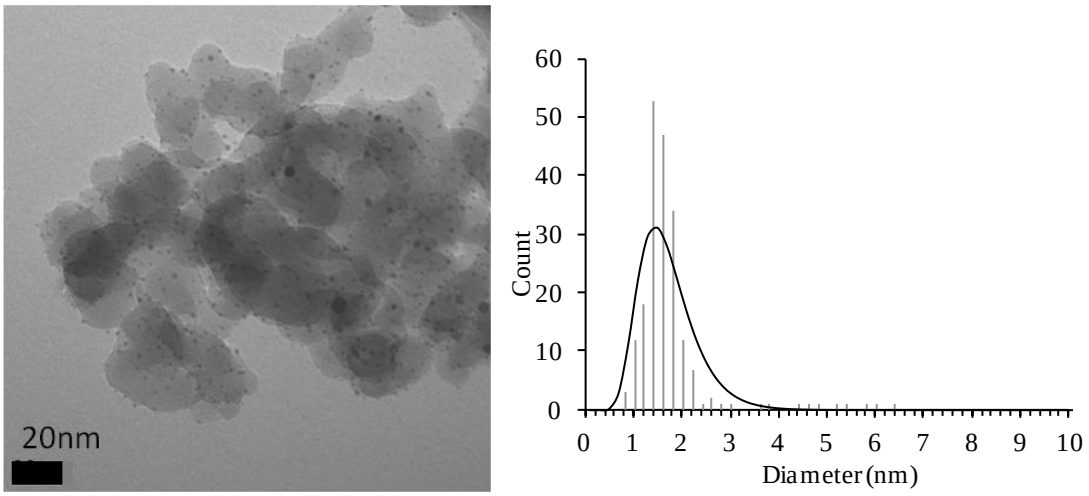

(COD)Pt(Me)(N(SiMe$_3$)$_2$)@SiO$_{2\text{-}700}$ treated under H_2 flow. 221 nanoparticles count. Mean size 1.7 (σ=0.8) nm.

G. (COD)Pt(Cl)(N(SiMe$_3$)$_2$)

Figure S15. IR-DRIFT

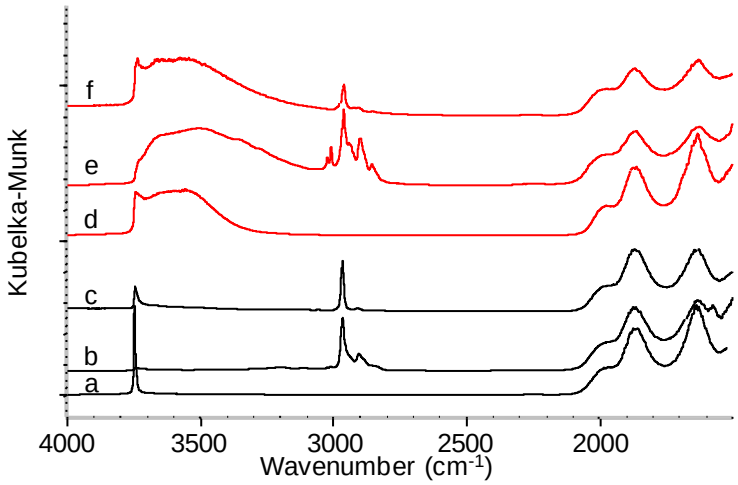

a) $SiO_{2\text{-}700,}$ b) (COD)Pt(Cl)(N(SiMe$_3$)$_2$)@$SiO_{2\text{-}700}$, c) after static H_2 treatment, d) $SiO_{2\text{-}200}$, e) (COD)Pt(Cl)(N(SiMe$_3$)$_2$)@$SiO_{2\text{-}200}$, f) after static H_2 treatment

	grafted	after H_2
$SiO_{2\text{-}700}$	3022/3008/2964/2934/2902/2888	2966/2907
$SiO_{2\text{-}200}$	3023/3009/2962/2942/2934/2900/2853	2964/2907

Figure S16.

Solid-state NMR of (COD)Pt(Cl)(N(SiMe$_3$)$_2$@SiO$_{2\text{-}200}$

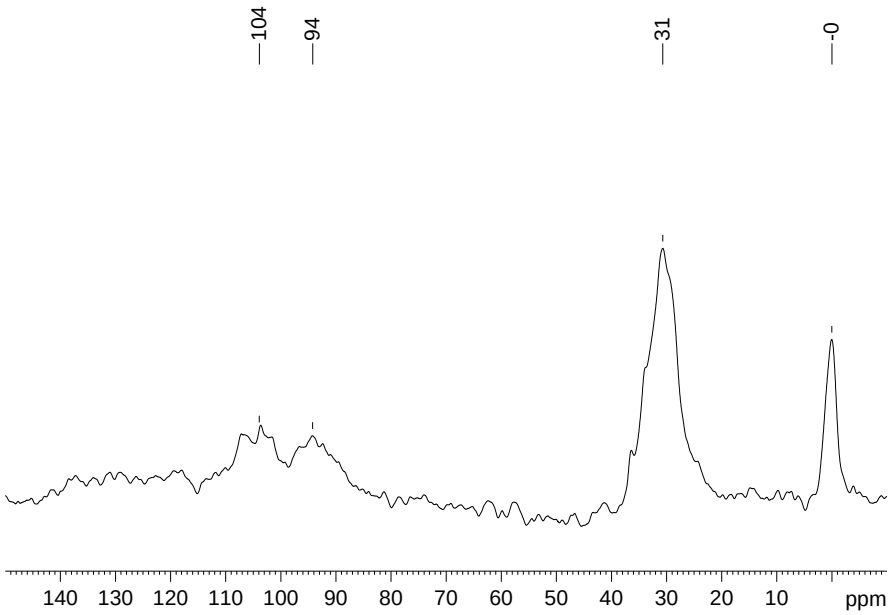

^{13}C CP/MAS solid state NMR spectra of (COD)Pt(Cl)(N(SiMe$_3$)$_2$)@SiO$_{2\text{-}200}$ (d1 = 14 s, 12312 scans, lb=100Hz)

Solid-state NMR of (COD)Pt(Cl)(N(SiMe$_3$)$_2$@SiO$_{2\text{-}700}$

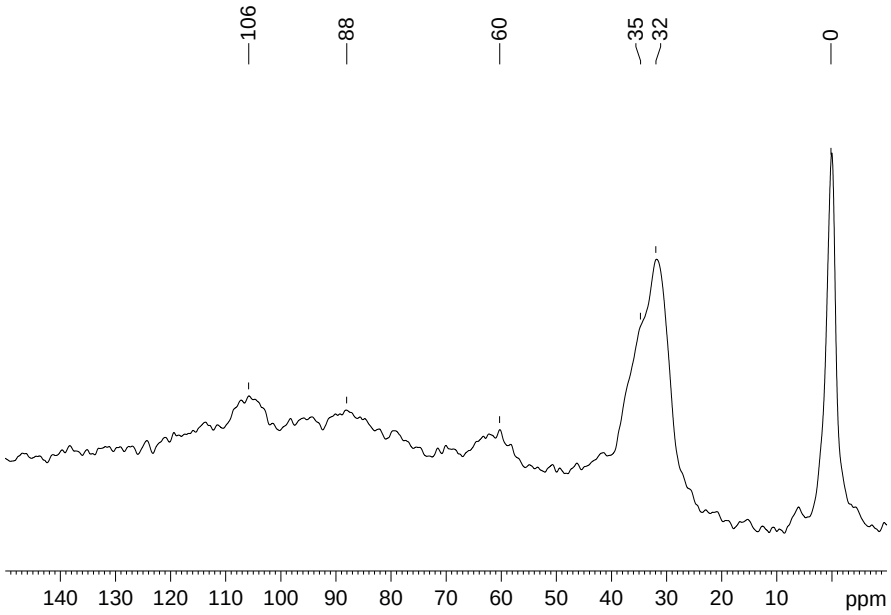

^{13}C CP/MAS solid state NMR spectra of (COD)Pt(Cl)(N(SiMe$_3$)$_2$)@SiO$_{2\text{-}700}$ (d1 = 4 s, 39207 scans, lb=100Hz)

Note: the additional peak at 60 ppm is attributed to physisorbed diethylether.

Figure S17. TEM

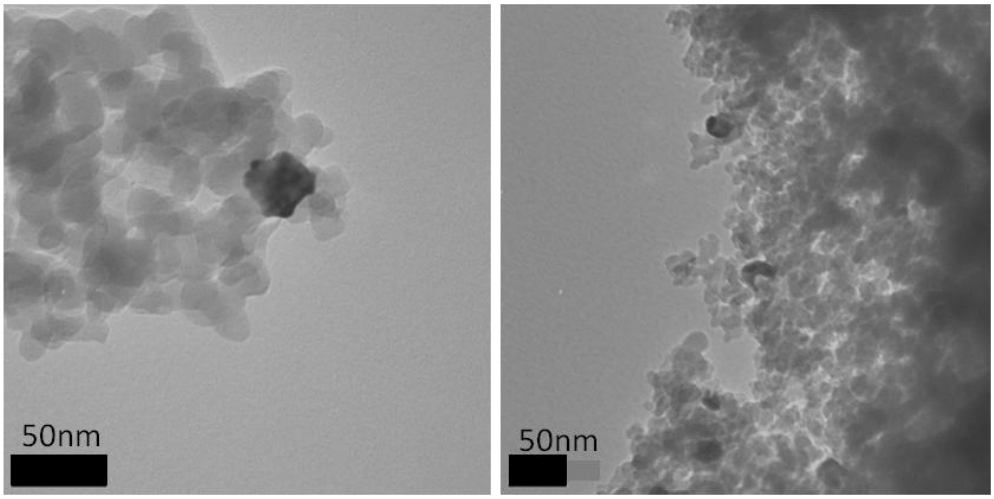

(COD)Pt(Cl)(N(SiMe$_3$)$_2$)@SiO$_{2\text{-}200}$ treated under static H_2 atmosphere.

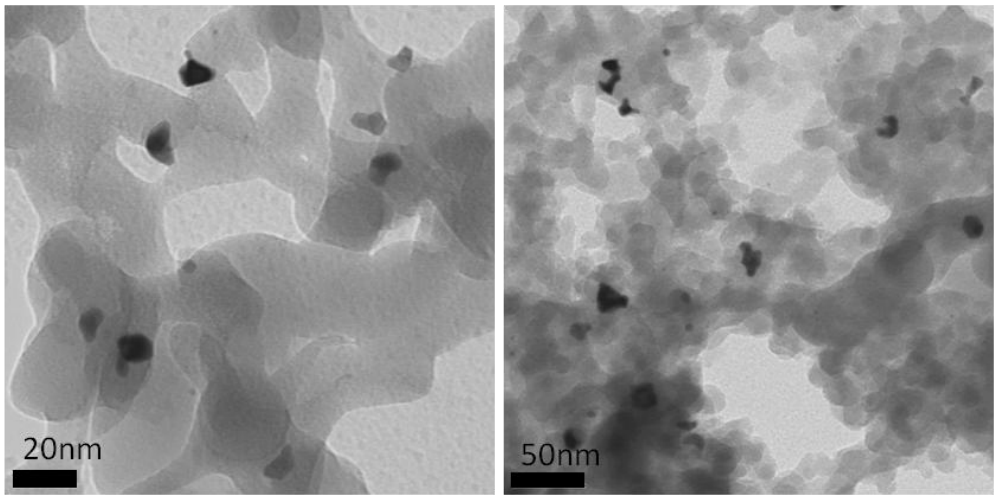

(COD)Pt(Cl)(N(SiMe$_3$)$_2$)@SiO$_{2\text{-}700}$ treated under static H_2 atmosphere.

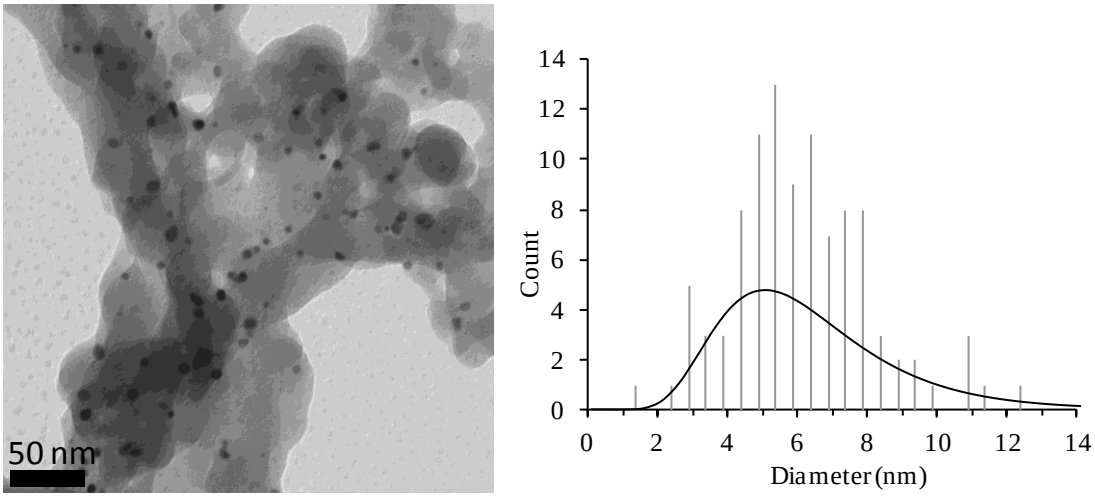

(COD)Pt(Cl)(N(SiMe$_3$)$_2$)@SiO$_{2\text{-}700}$ treated under H_2 flow. 103 nanoparticles count. Mean size 6.3 (σ=2.4) nm.

This journal is © The Royal Society of Chemistry 2012

H. (COD)Pt(OSi(O*t*Bu)$_3$)(N(SiMe$_3$)$_2$)

Figure S18. Liquid state NMR of 3 (COD)Pt(OSi(OtBu)$_3$)(N(SiMe$_3$)$_2$) in C_6D_6.

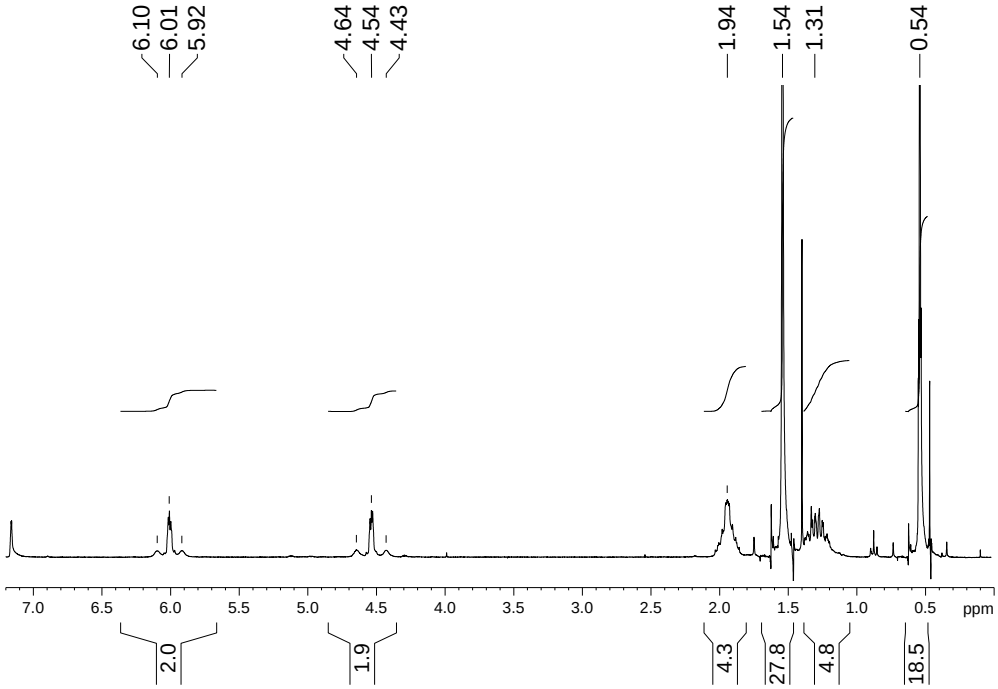

^{1}H NMR , d1=1sec, 8 scans.

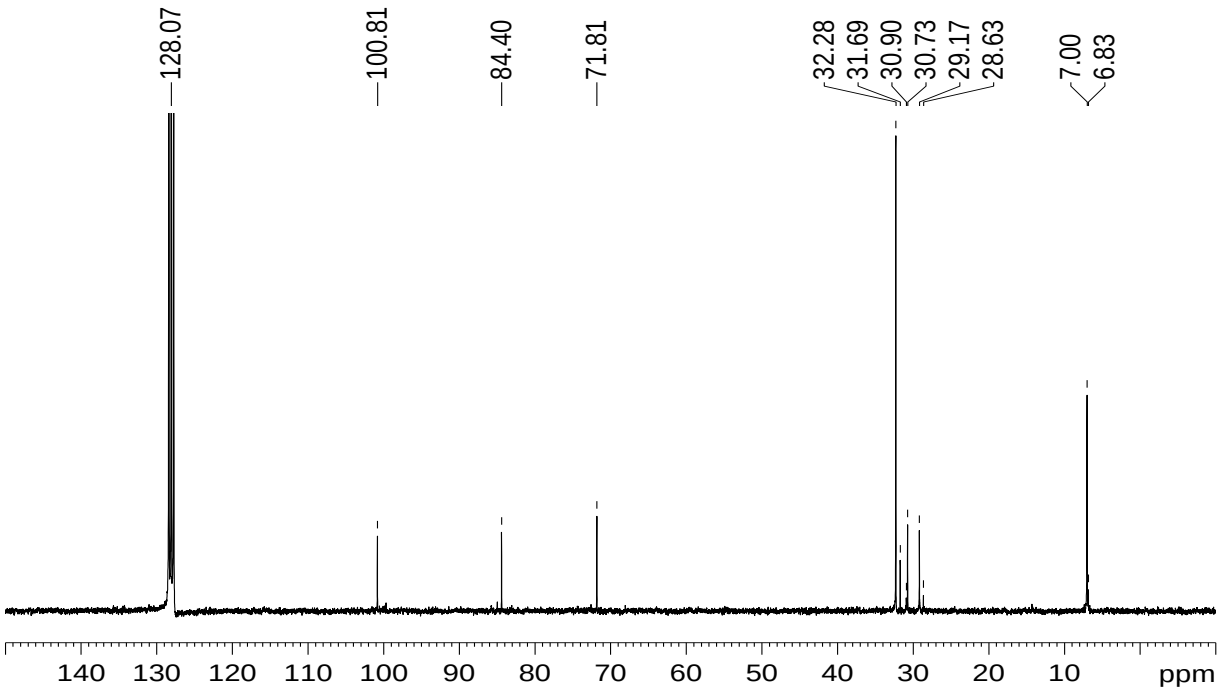

^{13}C NMR, d1=1sec, 1875 scans.

^{1}H NMR (C6D6; δ, ppm): 0.54 (s, 18H, -Si*Me$_3$*), 1.31 (m, 4H, endo C*H$_2$*), 1.54 (s, 27H, OC*Me$_3$*), 1.94 (m, 4H, exo C*H$_2$*), 4.55 (t, 2H, =C*H*, trans to OSi, JPt-H=66 Hz), 6.01 (t, 2H, =C*H*, trans to N, JPt-H=51Hz).

^{13}C NMR (C6D6; δ, ppm): 6.8 (s, OC*Me*$_3$), 7.0 (s, Si*Me*$_3$), 29.2 (s, *C*H$_2$), 30.7 (s, *C*H$_2$, COD), 32.3 (s, OC*Me*$_3$), 71.8 (s, O*C*Me$_3$), 84.4 (s, =CH, trans to OSi), 100.8 (s, =CH, trans to N).

Figure S19. IR-DRIFT

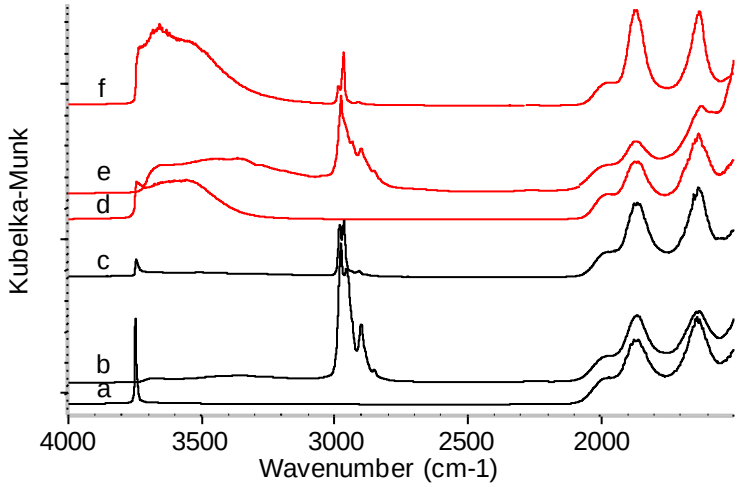

a) $SiO_{2\text{-}700,}$ b) (COD)Pt(OSi(O*t*Bu)$_3$)(N(SiMe$_3$)$_2$)@$SiO_{2\text{-}700}$, c) after static H_2 treatment, d) $SiO_{2\text{-}200}$, e) (COD)Pt(OSi(O*t*Bu)$_3$)(N(SiMe$_3$)$_2$)@$SiO_{2\text{-}200}$, f) after static H_2 treatment

	grafted	after H_2
$SiO_{2\text{-}700}$	2976/2956/2951/2899/2851	2981/2965/2909
$SiO_{2\text{-}200}$	2977/2958/2933/2900/2852	2983/2964/2906

This journal is © The Royal Society of Chemistry 2012

Figure S20.

Solid-state NMR of (COD)Pt(N(SiMe$_3$)$_2$)(OSi(OtBu)$_3$)@SiO$_{2\text{-}200}$

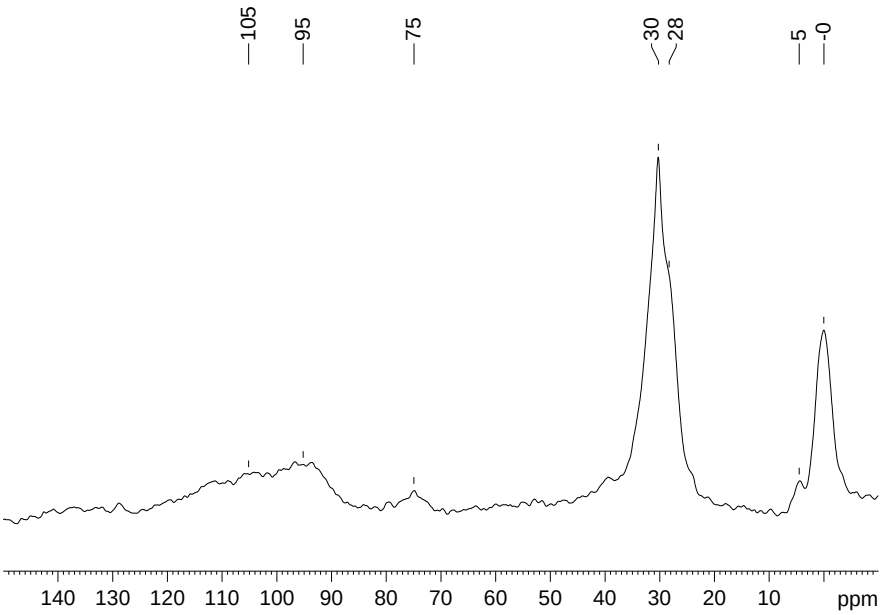

^{13}C CP/MAS solid state NMR spectra of (COD)Pt(N(SiMe$_3$)$_2$)(OSi(O*t*Bu)$_3$)@SiO$_{2\text{-}200}$ (d1 = 4 s, 12490 scans, lb=100Hz)

Solid-state NMR of CODPt(N(SiMe$_3$)$_2$)(OSi(OtBu)3)@SiO$_{2\text{-}700}$

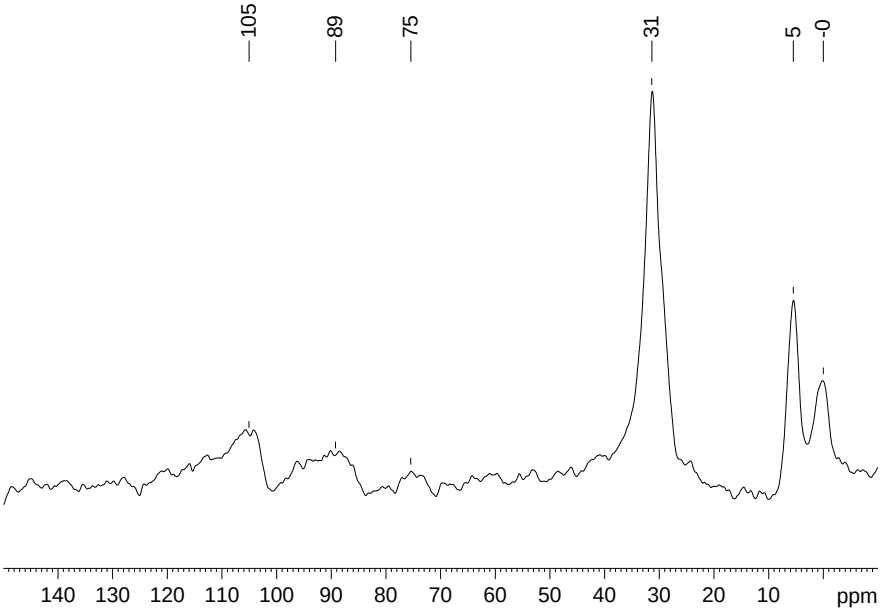

^{13}C CP/MAS solid state NMR spectra of CODPt(N(SiMe$_3$)$_2$)(OSi(O*t*Bu)$_3$)@SiO$_{2\text{-}700}$ (d1 = 2 s, 10416 scans, lb=100Hz)

This journal is © The Royal Society of Chemistry 2012

Figure S21. TEM

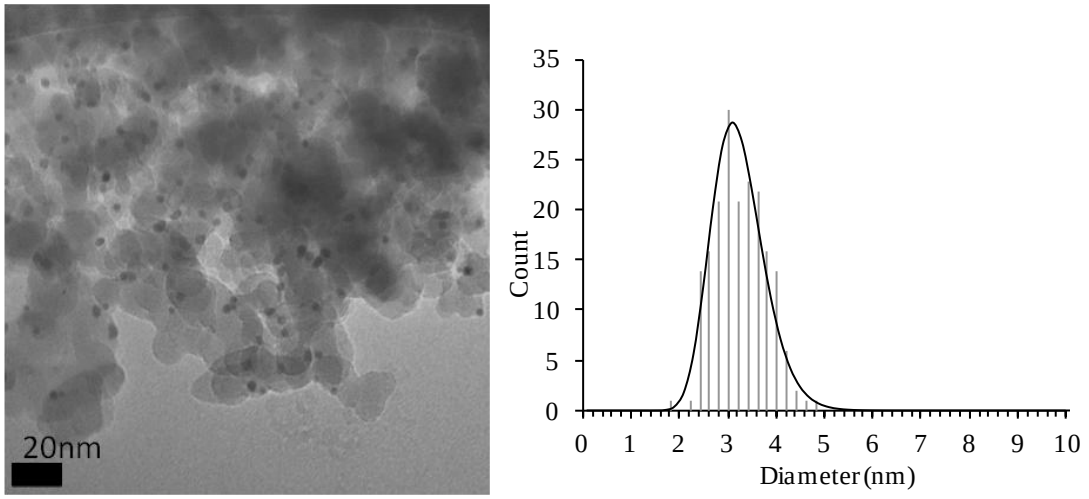

(COD)Pt(OSi(O*t*Bu)$_3$)(N(SiMe$_3$)$_2$)@SiO$_{2\text{-}200}$ treated under static H_2 atmosphere. 189 nanoparticles count. Mean size 3.2 (σ=0.5).

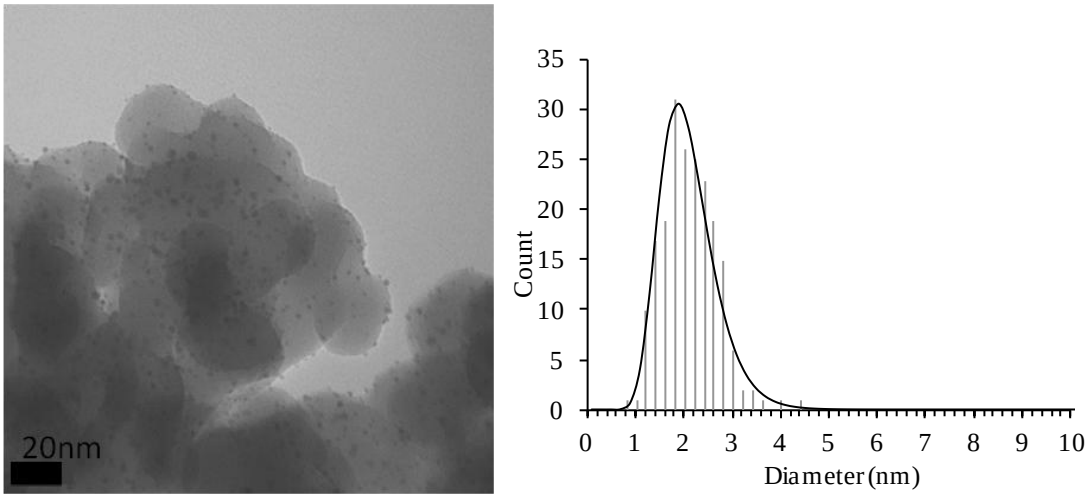

(COD)Pt(OSi(OtBu)$_3$)(N(SiMe$_3$)$_2$)@SiO$_{2\text{-}700}$ treated under static H_2 atmosphere. 200 nanoparticles count. Mean size 2.1 (σ=0.6).

I. HOSi(O*t*Bu)$_3$

For the methyl-siloxy complexes grafting, IR-DRIFT reveals the presence of *t*Bu units on the surface, to address the question whether the silanol is absorbed or grafted on the surface, $SiO_{2\text{-}700}$ was contacted with 1.2 equivalents of tris(tert-butoxy)silanol in pentane for 3 hours followed by multiple washings and secondary vacuum drying, mimicking the full process of a grafting procedure. Typical *t*Bu ν(C-H) vibrations at 2982, 2938, 2912 and 2877 cm^{-1} are observed by IR-DRIFT. A large IR-band is observed at 3360 cm^{-1} and can be attributed to the silanol of absorbed tris(tert-butoxy)silanol. By ^{13}C SS-NMR the $C(CH_3)_3$ and $C(CH_3)_3$ are respectively found at 71 and 30 ppm.

After treatment under H_2 under static atmosphere *t*Bu unit are still present at the surface as demonstrated by IR-DRIFT spectroscopy and consumption of surface OH is evidenced by the intensity diminution of the band at 3747 cm^{-1}. Those observations indicates the probable formation of SiO bonds thus anchoring the tris(tert-butoxy)silanol to the surface.

Figure S22. Solid-state NMR of HOSi(OtBu)$_3$ absorbed onto SiO$_{2\text{-}700}$

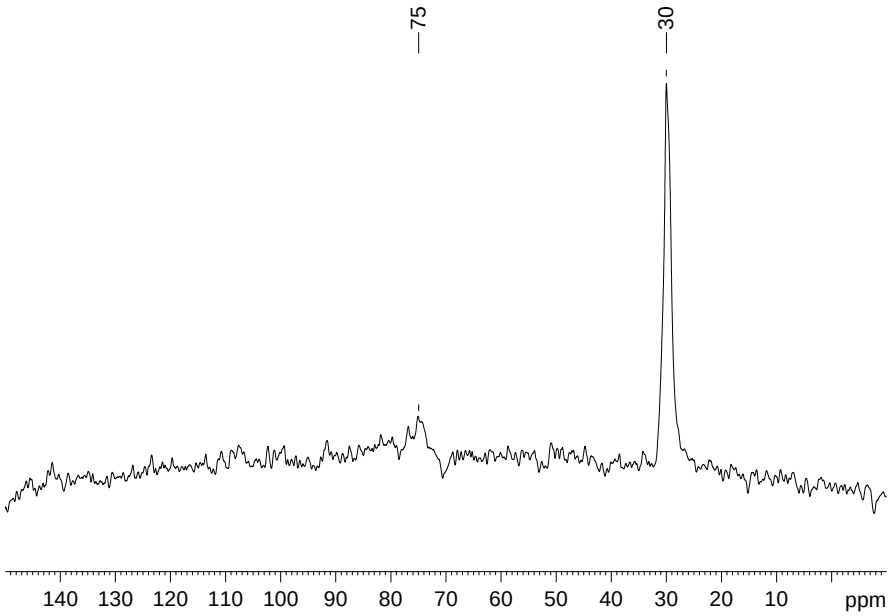

^{13}C CP/MAS solid state NMR spectra of HOSi(O*t*Bu)$_3$@$SiO_{2\text{-}700}$ (d1 = 2 s, 28529 scans, lb=100Hz)

Figure S23. IR-DRIFT

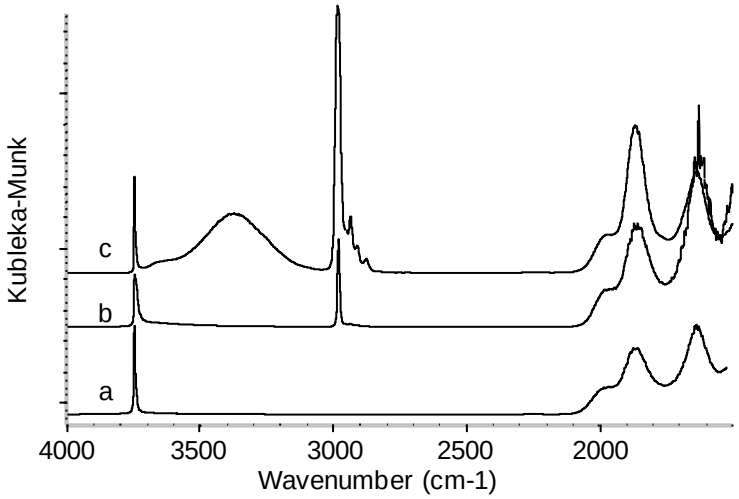

a) $SiO_{2\text{-}700}$, b) after static H_2 treatment, c) $HOSiO(t\text{Bu}_3)_3@SiO_{2\text{-}700}$

	grafted	after H_2
$SiO_{2\text{-}700}$	3370/2983/2937/2911/2878	3747/2983

Figure S24

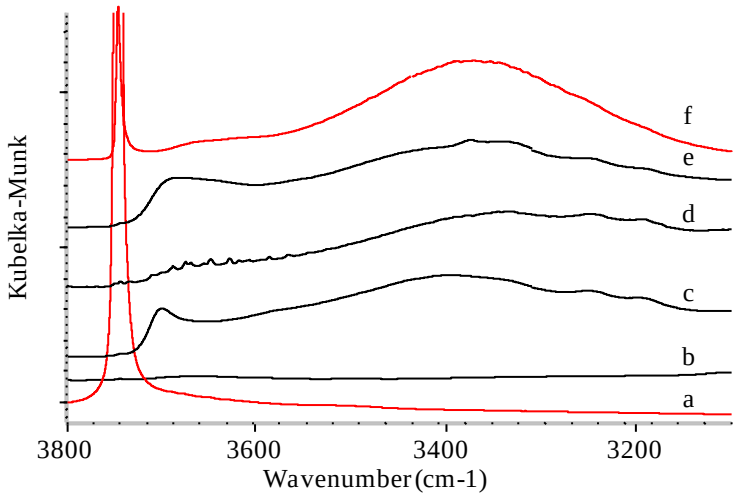

IR-DRIFT spectra of a) $SiO_{2\text{-}700}$ b) $(COD)Pt(Me)(N(SiMe_3)_2@SiO_{2\text{-}700}$, c) $(COD)Pt(OSi(O\text{Bu})_3)_2@SiO_{2\text{-}700}$, d) $(COD)Pt(Me)(OSi(O\text{Bu})_3)@SiO_{2\text{-}700}$, e) $(COD)Pt(OSi(O\text{Bu})_3)(N(SiMe_3)_2@SiO_{2\text{-}700}$, f) $HOSi(O\text{Bu})_3@SiO_{2\text{-}700}$ (smaller Y scale).

J. ^{13}C SS-NMR spectra of Pt complexes grafted onto $SiO_{2\text{-}200}$.

Figure S25.

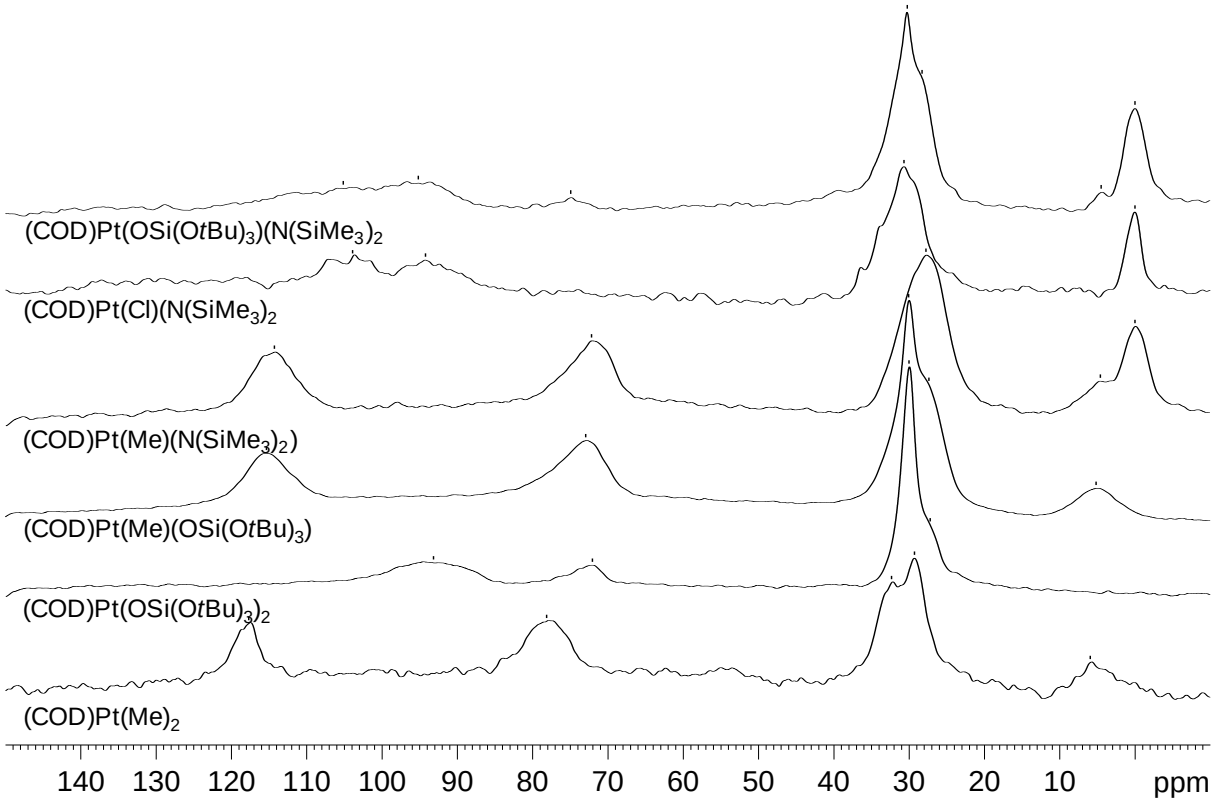

K. Maximum surface coverage for (COD)Pt(R)(OSi≡) species

Table S2.

The maximum radius of the grafted molecule is determined from DRX data of (COD)Pt(R)(OSi(O*t*Bu)$_3$) when available. For (COD)Pt(Cl)(OSi≡) the measure is derived from the (COD)Pt(CH_3)(OSi(O*t*Bu)$_3$) complex, considering the carbon atom of the methyl ligand as a chlorine atom. We consider the molecules as discs in dense packing, with a surface density of 0.9069.

R	radius Å	disc surface nm^2	$Pt.nm^{-2}$
Me	0.37	0,43	2,6
Cl	0.36	0,40	2,8
OSi(OtBu)3	0.60	1,12	1,0
N(SiMe3)2	0.52	0,83	1,3